Digest Journal of Nanomaterials and Biostructures Vol. 20, No. 4, October-December 2025, p. 1217-1222

Enhanced photoelectrochemical water-splitting of TiO_2 electrode by $NiWO_4$-WO_3 decoration

S. Wannapop *, C. Keeprawat, T. Chuebang, T. Ninsu, A. Somdee
Faculty of Science, Energy, and Environment, King Mongkut's University of Technology North Bangkok, Rayong Campus, Rayong 21120, Thailand

The NWO_4-WO_3/TiO_2 and $NiWO_4$-WO_3 heterostructures were created via a hydrothermal process at 160°C for 12 hours. The samples were analyzed using XRD, XPS, SEM, EDS, TEM, HRTEM, and a UV-Vis spectrophotometer (UV-Vis). The energy bandgap of pristine TiO_2 decreased after enhancement with $NiWO_4$–WO_3. The samples served as photoanodes in PEC water-splitting cells, with NWO-WO-TiO_2 outperforming both pristine TiO_2 and $NiWO_4$-WO_3 under solar simulation. EIS revealed that the NWO-WO-TiO_2 material's charge carrier and transport were improved.

(Received July 19, 2025; Accepted October 8, 2025)

Keywords: PEC, XRD, WO_3, SEM, $NiWO_4$

1. Introduction

Economic, geopolitical, and environmental factors are central to the issue of energy shortages. Rapid industrialization in emerging economies places significant pressure on global energy markets, while geopolitical tensions can disrupt the flow of essential resources. Additionally, the need to transition to renewable energy sources to combat climate change adds urgency to this situation. Adopting renewable energy brings various benefits beyond environmental sustainability.

PEC water splitting uses sunlight and water to produce clean hydrogen fuel without greenhouse gas emissions [1]. Although it has great potential, several challenges persist, including improving the efficiency and stability of photoelectrodes, reducing material costs, and scaling the technology for commercial applications. Although it has great potential, several challenges persist, including improving the efficiency and stability of photoelectrodes, reducing material costs, and scaling the technology for commercial applications [2]. As a semiconductor, TiO_2 possesses unique properties such as high stability, abundance, and advantageous band gap characteristics, making it an ideal candidate for facilitating the PEC process [3]. TiO_2 has become crucial for developing efficient and environmentally friendly energy systems because it captures sunlight and converts it into chemical energy. However, its effectiveness in PEC systems is limited by several factors, including a low light absorption coefficient and decreased charge carrier mobility [4]. Researchers have explored strategies to address these drawbacks, such as using heterojunctions with semiconductors doped with metal or non-metal elements, heterostructures, and plasmonic enhancement [5]. The heterostructure enhances TiO_2 by improving light absorption, charge separation, and band alignment through the use of other semiconductors, such as CdS [6], ZnS [7], $BiVO_4$ [8], $SrTiO_3$ [9], Bi_2WO_6 [10], WO_3 [11], $CoWO_4$ [12], and $NiWO_4$ [13]. WO_3 and $NiWO_4$ [14-16] are excellent materials for PEC applications due to their complementary properties, which enhance photocatalytic activity through a narrow bandgap, high stability, efficient charge transport, and Oxidation Capability. The combination of WO_3 and $NiWO_4$ enhances the efficiency of TiO_2. WO_3 serves as an electron-transporting layer, while $NiWO_4$ adds extra light absorption and provides catalytic sites. This heterostructure promotes efficient water oxidation and hydrogen evolution, effectively addressing the limitations of each material when used alone.

In this study, we modified TiO_2 with $NiWO_4$-WO_3 on its surface using a hydrothermal process and characterized the samples through various methods. The $NiWO_4$-WO_3/TiO_2 and TiO_2 nanostructures were utilized as photoanodes for PEC water-splitting applications.

* Corresponding author: surangkana.w@sciee.kmutnb.ac.th
https://doi.org/10.15251/DJNB.2025.204.1217

2. Experiment

$NiWO_4$-WO_3 (NWO-WO) and $NiWO_4$-WO_3/TiO_2 (NWO-WO-TiO_2) heterostructures were synthesized via the hydrothermal method. To prepare the solution, 0.5 g of titanium dioxide (P25), 0.5 mmol of $Na_2WO_4 \cdot 2H_2O$, and $Ni(NO_3)_2$ was dissolved in 20 mL of DI water with vigorous stirring for 10 min. The pH was adjusted to 7 with 3 M NaOH and HCl, then the mixture was hydrothermally synthesized at 160 °C for 1 hour. It was washed with DI water and ethanol, dried at 60 °C for 24 h., and calcined at 600 °C for 1 h. Characterization was performed using SEM, TEM, XRD, and UV-vis reflectance.

PEC water splitting measurements and electrochemical impedance spectroscopy were conducted under an AM 1.5 solar simulator.

TiO_2 and modified TiO_2 photoanodes were prepared using the sol-gel method, mixing a metal oxide: PEG ratio of 1:0.45 dissolved in a 1 ml mixed solution (water: ethanol, 1:1) and stirred for 30 min. The gel was applied on a 1 cm x 1 cm surface and calcined at 500 °C for 1 h.

3. Results and discussion

The XRD patterns in Fig. 1 show TiO_2, NWO-WO, and NWO-WO-TiO_2, with TiO_2 exhibiting anatase (JCPDS No. 21-1272) [17] and rutile (JCPDS No. 21-1276) [18] phases. The NWO-WO pattern includes WO_3 (JCPDS No. 05-0363) [19] and $NiWO_4$ (JCPDS No. 15-0755) [20] phases. Moreover, the diffraction pattern of the NWO-WO-TiO_2 nanostructures is similar to that of TiO_2, but the $NiWO_4$ and WO_3 patterns are also present. Fig. 1(b) shows the XPS spectrum for TiO_2, NWO-WO, and NWO-WO-TiO_2. TiO_2 has peaks for Ti 2p and O 1s, while NWO-WO displays W 4f, O 1s, and Ni 2p peaks. NWO-WO-TiO_2 features peaks for W 4f, Ti 2p, O 1s, and Ni 2p.

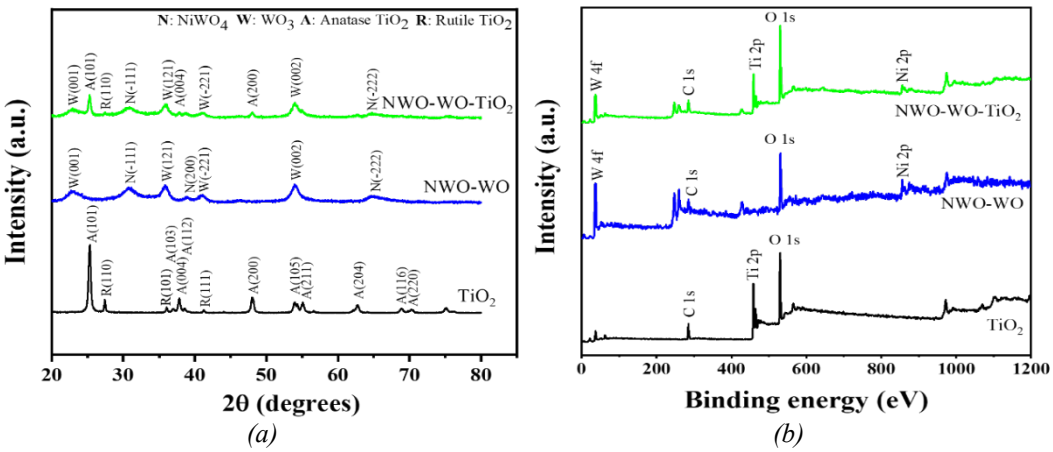

Fig. 1. XRD patterns of TiO_2, NWO-WO, and NWO-WO-TiO_2, respectively.

The high-resolution (HR) spectrum in Fig. 2(a) shows the W $4f_{7/2}$ and W $4f_{5/2}$ signals for the NWO-WO-TiO_2 sample at 35.90 and 37.98 eV, respectively. The NWO-WO sample exhibits these signals at 35.95 eV and 38.11 eV, both of which correspond to W^{6+} ions [21]. Fig. 2(b) shows the Ni $2p_{3/2}$ and Ni $2p_{1/2}$ signals for NWO-WO-TiO_2 at 856.01 and 873.65 eV. NWO-WO positions are found at 856.35 and 873.94 eV, respectively, corresponding to Ni^{2+} ions [21]. In Fig. 2(c), the Ti $2p_{3/2}$ and Ti $2p_{1/2}$ peaks for the NWO-WO-TiO_2 sample appear at 450.10 and 464.76 eV, respectively, whereas TiO_2 exhibits peaks at 458.76 and 464.44 eV, characteristic of Ti^{4+} ions [22]. The shift in the Ti $2p_{3/2}$ position for NWO-WO-TiO_2 suggests the formation of Ti^{3+} ions due to the addition of $NiWO_4$ and WO_3. The O 1s signals for NWO-WO-TiO_2 shown in Fig. 2(d) exhibit peaks at 530.40 (Ti-O in TiO_2), 531.34 (O^{2-} in $NiWO_4$), 532.27 (C-O-H), and 533.32 eV (adsorbed oxygen

in WO_3). The NWO-WO peaks at 531.03 indicate O^{2-} in $NiWO_4$, while peaks at 532.51 and 533.45 eV represent C-O-H and adsorbed oxygen in WO_3. The TiO_2 signals at 529.88 and 532.02 eV correspond to Ti-O and O-H groups, respectively [23-25].

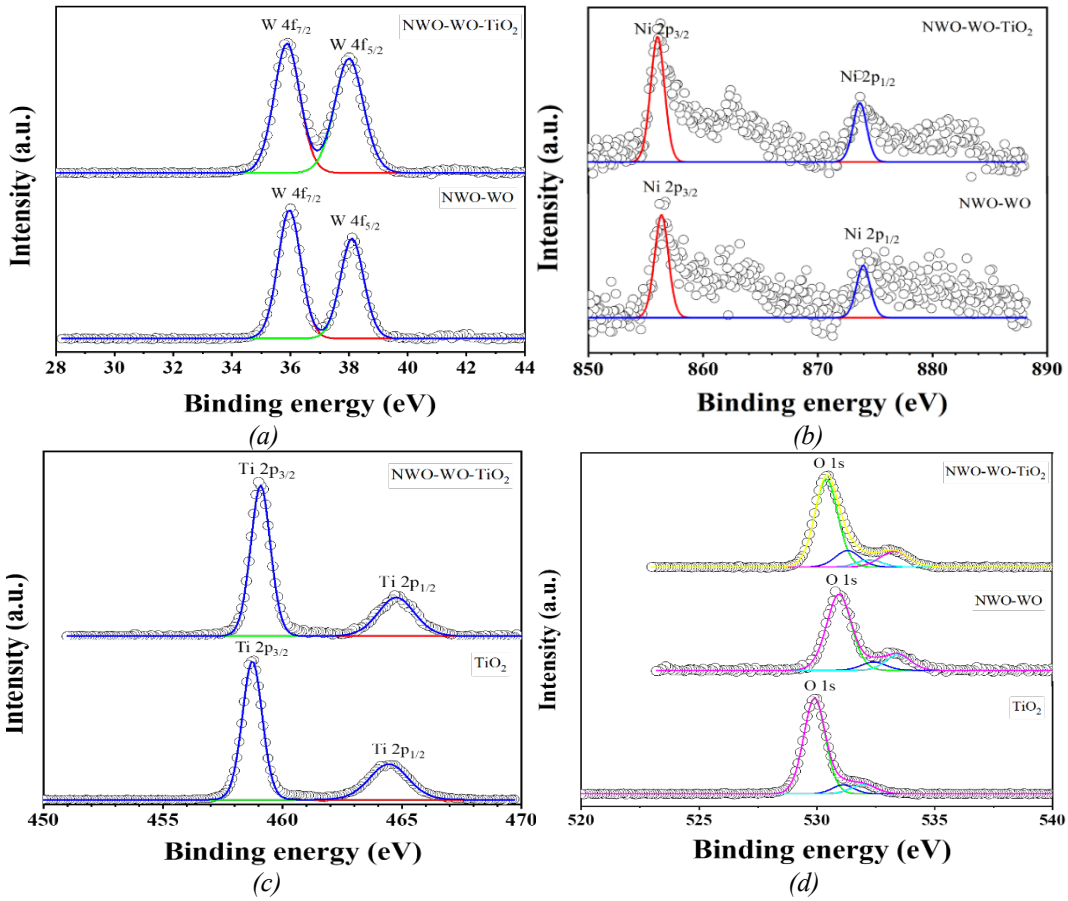

Fig. 2. HR XPS of W 4f and Ni 2p for NWO-WO and NWO-WO-TiO_2 (a-b), Ti 2p for NWO-WO-TiO_2 and TiO_2 (c), and O 1s for NWO-WO-TiO_2, NWO-WO, and TiO_2 (d).

Fig. 3 shows an SEM image of TiO_2, NWO-WO, and NWO-WO-TiO_2 nanostructures, confirming the successful deposition of TiO_2 nanoparticles onto NiWO-WO and examining their morphology and distribution.

Fig. 4 presents the TEM images of TiO_2, NWO-WO, and NWO-WO-TiO_2. The particle size of TiO_2 nanoparticles ranges from 20 to 100 nm, while NWO-WO has a polygonal shape and a diameter of approximately 200-400 nm. Additionally, NWO-WO-TiO_2 consists of TiO_2 nanoparticles decorated on the surface of $NiWO_4$-WO_3. Fig. 4(d) shows the HRTEM image of NWO-WO-TiO_2, which displays the d-spacing measurements of Rutile TiO_2, $NiWO_4$, and WO_3 particles, recorded at 0.27 nm, 0.23 nm, and 0.25 nm for the (110), (200), and (121) planes, respectively. The HRTEM analysis confirmed the presence of $NiWO_4$, WO_3, and TiO_2 in the heterojunction formed by $NiWO_4$-WO_3/TiO_2, as supported by EDX and XPS results.

Fig. 5a shows that adding $NiWO_4$-WO_3 enhances light absorption in TiO_2. The band gap energies are about 3.6, 3.2, and 3.5 eV for TiO_2, NWO-WO, and NWO-WO-TiO_2, respectively, showing a smaller band gap for NWO-WO-TiO_2 compared to TiO_2.

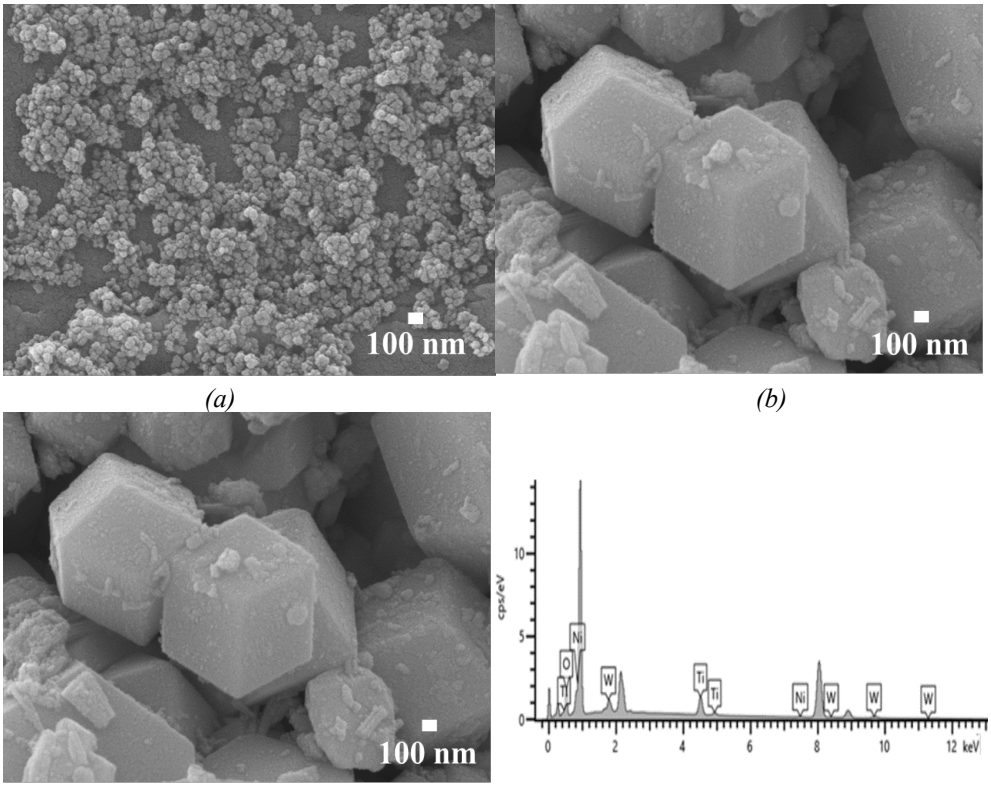

Fig. 3. SEM image and EDX of TiO_2 (a), NWO-WO (b), and NWO-WO-TiO_2 (c-d), respectively.

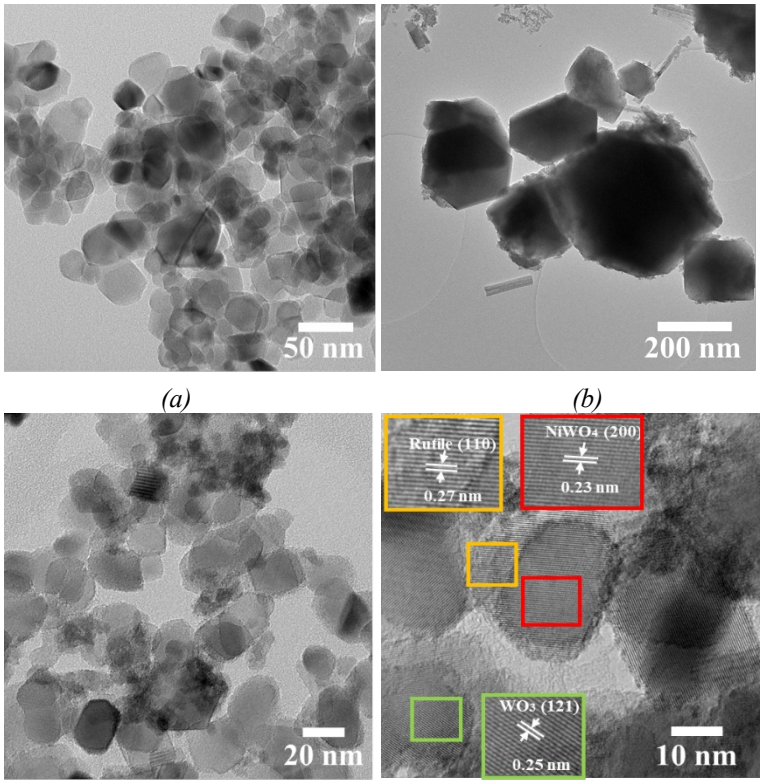

Fig. 4. TEM image and HRTEM image of TiO_2 (a), NWO-WO (b), and NWO-WO-TiO_2 (c-d), respectively.

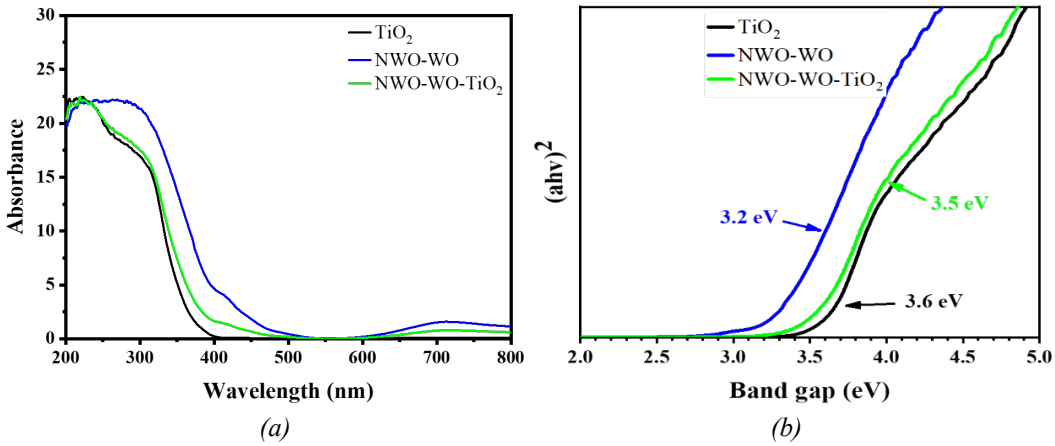

Fig. 5 shows UV-vis and Tauc plots of TiO_2, NWO-WO, and NWO-WO-TiO_2.

Fig. 6 shows the LSV and Nyquist plots for TiO_2, NWO-WO, and NWO-WO-TiO_2. The addition of $NiWO_4$-WO_3 significantly enhanced the performance of the TiO_2 photoanode, improving light absorption and surface area. NWO-WO-TiO_2 achieved the highest I_{sc} of 3.98 mA/cm² at 1.2 V. The Nyquist plot in Fig. 6b indicates that NWO-WO-TiO_2 has the smallest arc radius, reflecting the lowest resistance among the tested photocathodes.

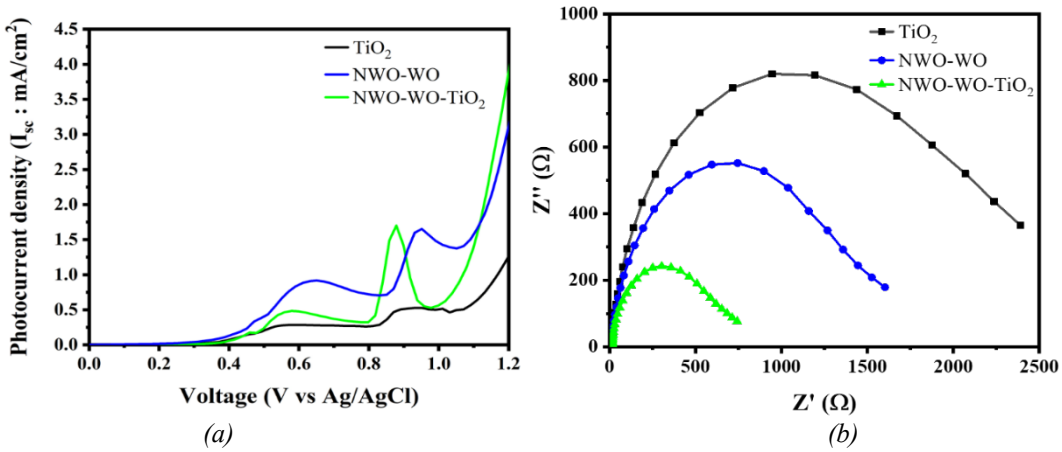

Fig. 6. (a) LSV, and (c) Nyquist plots of TiO_2, NWO-WO, NWO-WO-TiO_2

4. Conclusions

TiO_2, NiWO-WO, and NiWO-WO-TiO_2 were successfully synthesized using the hydrothermal method. NWO-WO-TiO_2 boosts PEC system performance by expanding light absorption into the visible range, enhancing charge transfer, and enabling synergistic effects between co-catalysts. This innovative approach addresses key challenges associated with PEC water splitting, including efficiency, stability, and scalability, thereby advancing the prospects of renewable hydrogen production.

Acknowledgments

This research was funded by King Mongkut's University of Technology North Bangkok. Contract no. KMUTNB-66-KNOW-08.

References

[1] Nabgan, W., et al., International Journal of Hydrogen Energy 52, 358-380 (2024); https://doi.org/10.1016/j.ijhydene.2023.05.162

[2] Zheng, J., et al., Energy and Environmental Science 12(8), 2345-2374 (2019); https://doi.org/10.1039/C9EE00524B

[3] Somdee, A., et al., Inorganic Chemistry Communications 134, 109013 (2021); https://doi.org/10.1016/j.inoche.2021.109013

[4] Sawal, M.H., et al., Electrochimica Acta 467, 143142. (2023); https://doi.org/10.1016/j.electacta.2023.143142

[5] Hamdani, I.R., A.N. Bhaskarwar, Renewable and Sustainable Energy Reviews 138, 110503 (2021); https://doi.org/10.1016/j.rser.2020.110503

[6] Chen, S., C. Li, and Z. Hou, International Journal of Hydrogen Energy 44(47), 25473-25485 (2019); https://doi.org/10.1016/j.ijhydene.2019.08.049

[7] Hassan, M.A., et al., Acta Materialia 146, 171-175 (2018); https://doi.org/10.1016/j.actamat.2017.12.063

[8] Somdee, A., et al., Journal of Alloys and Compounds 937, 168434. (2023); https://doi.org/10.1016/j.jallcom.2022.168434

[9] Bashiri, R., et al., International Journal of Hydrogen Energy 46(48), 24607-24619 (2021); https://doi.org/10.1016/j.ijhydene.2020.02.106

[10] Keeprawat, C., A. Somdee, S. Wannapop. 2022 International Conference on Power, Energy and Innovations (ICPEI) (2022); https://doi.org/10.1109/ICPEI55293.2022.9986891

[11] Pinto, F., et al., The Journal of Physical Chemistry C 126(2), 871-884 (2022); https://doi.org/10.1021/acs.jpcc.1c08403

[12] Chatterjee, P., A.K. Chakraborty, Solar Energy 232, 312-319 (2022); https://doi.org/10.1016/j.solener.2021.12.075

[13] Fan, L., et al., International Journal of Hydrogen Energy 47(46), 20153-20165 (2022); https://doi.org/10.1016/j.ijhydene.2022.04.148

[14] Zhu, J., et al., Electrochimica Acta 112,191-198 (2013); https://doi.org/10.1016/j.electacta.2013.08.146

[15] Do, T.H., et al., Nano Energy 23, 153-160 (2016); https://doi.org/10.1016/j.nanoen.2016.03.021

[16] Ji, Y., et al., ACS Sustainable Chemistry & Engineering 6(8), 9555-9559 (2018); https://doi.org/10.1021/acssuschemeng.8b01841

[17] Wannapop, S., et al., Digest Journal of Nanomaterials & Biostructures (DJNB) 19(3) 999-1007 (2024); https://doi.org/10.15251/DJNB.2024.193.999

[18] Panchakhant, P., et al., Ceramics International 50(18), Part A): 32748-32754 (2024); https://doi.org/10.1016/j.ceramint.2024.06.084

[19] Subramani, T., et al., Inorganic Chemistry Communications 142, 109709 (2022); https://doi.org/10.1016/j.inoche.2022.109709

[20] Pavithra, N.S., et al., Inorganic Chemistry Communications 157, 111346 (2023); https://doi.org/10.1016/j.inoche.2023.111346

[21] Srirapu, V.K.V.P., et al., Electrochimica Acta 209, 75-84 (2016); https://doi.org/10.1016/j.electacta.2016.05.042

[22] Singaram, B., et al., Ionics 25(2), 773-784 (2019); https://doi.org/10.1007/s11581-018-2628-x

[23] Martinez-Oviedo, A., et al., Progress in Natural Science: Materials International 31, (2021); https://doi.org/10.1016/j.pnsc.2021.02.001

[24] Daemi, S., et al., Journal of Electroanalytical Chemistry 848, 113270 (2019); https://doi.org/10.1016/j.jelechem.2019.113270

[25] Tong, M., et alJournal of Materials Science 54, (2019);